Spectral gap induced by structural corrugation in armchair graphene nanoribbons

S. Costamagna, O. Hernandez, and A. Dobry
Instituto de Física Rosario, Consejo Nacional de Investigaciones Científicas y Técnicas, Universidad Nacional de Rosario, Rosario, Argentina

(Received 7 January 2010; revised manuscript received 17 February 2010; published 12 March 2010)

We study the effects of the structural corrugation or rippling on the electronic properties of undoped armchair graphene nanoribbons (AGNRs). First, reanalyzing the single corrugated graphene layer we find that the two inequivalent Dirac points (DPs) move away from each other. Futhermore, the Fermi velocity v_F decreases when the rippling increases. Regarding the AGNRs, whose metallic behavior depends on their widths, we analyze, in particular, the case of the zero-gap band-structure AGNRs. By solving the Dirac equation with adequate boundary conditions we show that, due to the shifting of the DP, a gap opens up in the spectra. This gap scales with the square of the rate between the height and the wavelength of the deformation. We confirm this prediction by an exact numerical solution of the finite width rippled AGNR. Moreover, we find that the quantum conductance, calculated by the nonequilibrium Green's function technique, vanishes when the gap opens up. The main conclusion of our results is that a conductance gap should appear for all undoped corrugated AGNR, independently of their widths.

DOI: 10.1103/PhysRevB.81.115421 PACS number(s): 73.22.Pr, 73.23.Ad, 72.10.Fk

I. INTRODUCTION

The spectacular interest that has raised from the recent isolation of an atomic Carbon layer, the graphene,[1] is based on the unusual dynamics the electrons have in this material. In graphene, the electrons behave as massless relativistic particles giving rise, for example, to a sequence of Hall plateaus quite different than the ones observed in two-dimensional (2D) electron systems confined in semiconductor heterojuntions. Also the transport properties are remarkable. The mobility of electrons in suspended graphene could be even higher than in any known semiconductor.[2] Even the existence of graphene as a two-dimensional atomic crystal and its stability under ambient conditions is a surprising fact. According to the Mermin-Wagner theorem, there should not be long-range crystalline order in two dimensions at finite temperature. Even more, a flexible membrane embedded in the three-dimensional space should be crumpled because of long-wavelength bending fluctuations. However, these fluctuations can be suppressed by anharmonic couplings between bending and stretching modes. As a result, crystalline membranes can exist but they should be rippled.[3] Indeed, ripples were observed in graphene.[4] It has been proposed that they should play an important role in its electronic properties.[5,6] In particular, intrinsic rippling has been proposed as one of the possible mechanisms for electron scattering to explain the variation in the resistivity with the number of charge carriers experimentally seen in graphene.[7]

Between the research areas of graphene, one of the most important is the study of nanoribbons where the sheets are cut with a particular pattern to manage the electrical properties. Depending on the type of the edges, they can be either in zigzag [zigzag graphene nanoribbon (ZGNR)] or armchair configurations. It is known that a tight-binding model predicts that ZGNRs are always metallic while armchair graphene nanoribbons (AGNRs) can be either metallic or semiconducting, depending on their widths.[8] However, experiments suggest that AGNRs are always insulating with a gap that scales with the inverse of their width.[9] It has been shown that a possible source for this behavior is the border reconstruction which turns the ribbons into a semiconducting state.[10]

The effect of the corrugation on the electronic properties of graphene has been studied in previous works by a tight-binding-type model[11] and by *ab initio* local-density approximation calculations.[12] The rippling induces a nonuniform gauge field whose effects have been analyzed by analogy with an applied magnetic field. In this sense, the apparition of pseudo-Landau levels (LL) in the spectra was predicted. Regarding nanoribbons, the effects of the rippling on the conductivity were analyzed in a model, which includes also the effect of the disorder produced by charged impurities.[13] Although this approach is quite realistic, it cannot isolate only the effect of the rippling in order to know the contribution of each perturbation separately. Therefore, in this work, our main purpose is to analyze the effect of the corrugation on the electronic structure and the transport properties of AGNRs. First, as a necessary previous step, we study the electronic properties of corrugated graphene layers. We reanalyze the condition for the appearance of a flat band associated with the zero LL. We show that a strong rippling on the sheet is necessary to produce such a flat band. Then, we focus on the armchair-border-type nanoribbons. Particularly we analyze the case of the zero-gap band-structure AGNRs. We show that due to rippling a spectral gap is opened up in otherwise conducting ribbons. We subsequently analyze the quantum conductance by the nonequilibrium Green's function technique[14] (NEGF) and show that the opening of the gap manifests in an insulating behavior of the undoped samples.

The paper is organized as follows. In Sec. II we provide a detailed explanation of the corrugation model adopted and we study the effect of the corrugation on the electronic spectrum of a graphene sheet. Then, in Sec. III we study the effect of the rippling on the electronic spectrum and the conduction properties of metallic AGNR. Finally, in Sec. IV we

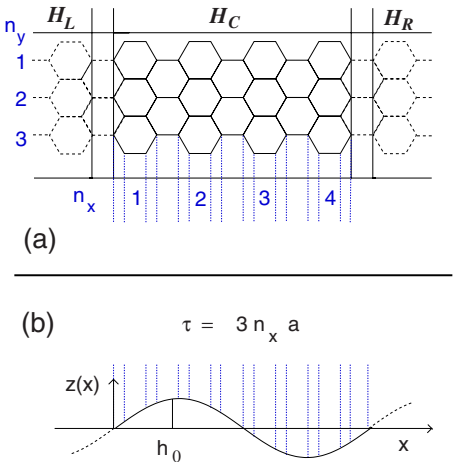

FIG. 1. (Color online) (a) Schematic view of an armchair graphene nanoribbon. The Hamiltonians labeled on top were used for the conductance calculations described in Sec. III B. In the central region $n_x=4$ and $n_y=3$, listed as indicated. (b) Side view in the x-z plane of the displacement of carbon atoms due to rippling. h_0 is the amplitude and τ the period.

present the conclusions of our paper and we discuss its implications.

II. EFFECT OF THE RIPPLING: THE GRAPHENE SHEET

Let us start by studying the effects of the corrugation on the electronic states for the case of a 2D graphene layer. This question was examined in a series of previous papers.[11,12] As it will be the starting point of our study of corrugated nanoribbons in the next section, we reanalyze this problem in the present section. This will be presented after a detailed description of the model adopted.

A. Model

We describe the electronic properties of the graphene layer by means of a tight-binding model with one π orbital for each carbon atom and nearest-neighbor hoppings between them. Carbon atoms arrange in a honeycomb lattice. It is not a Bravais lattice but can be constructed from the hexagonal lattice by putting a basis of two atoms. The hexagonal lattice can be constructed as $\mathbf{R}^{\mathbf{l}}=l_x\mathbf{a}_1+l_y\mathbf{a}_2$ with l_x and l_y integers, $\mathbf{a}_1=\frac{a}{2}(3,\sqrt{3})$ and $\mathbf{a}_2=\frac{a}{2}(3,-\sqrt{3})$ the primitive vectors. The basis is given by the atom A situated at $\mathbf{R}^{\mathbf{l}}$ and B at $\mathbf{R}^{\mathbf{l}}+\frac{a}{2}(1,\sqrt{3})$. $a\approx 1.41$ Å is the lattice constant and hereafter will be taken as unit of distance.

The corrugation was included as a sinusoidal function which modulates the z coordinate of each lattice site. The x and y coordinates are kept in their original values in the honeycomb lattice. For simplicity, we assume that the rippling depends only on the x direction (see Fig. 1 for the case of a nanoribbon). Then, the adopted $z(x)$ function reads

$$z(x)=h_0\sin\left(\frac{2\pi}{\tau}x\right), \tag{1}$$

where h_0 is the amplitude and τ the period of the rippling. This simple model for the corrugation has been used in previous works.[11,12] Since a superposition of functions of the type in Eq. (1) with different wave vectors and different amplitudes could generate a quite general corrugation, our study should be taken as a starting point for the effect of a general corrugation function. Furthermore, as our goal is the study of a nanoribbon whose length is large compared to its width, the one-dimensional character of the rippling function is justified.

The modulated structure induces a spatial variation in the hopping parameter t, being now dependent on the distance between the atoms. Developing t up to first order in the perturbed distance between the nearest neighbor (Δa) we have

$$t=t_0+\frac{t_0}{a}\alpha\Delta a,$$

$$\Delta a=\sqrt{a+[z(x)-z(x')]^2}-a, \tag{2}$$

where $t_0\approx 2.66$ eV is the hopping parameter of the undeformed graphene which is taken as a unit of energy in the present work. $\alpha=\frac{\partial \log t}{\partial \log a}\sim 2$, whose value is taken from Ref. 2. The rippling also produces a bending of the p orbitals. However it has been shown that the relative change in the hopping due to the bending is weaker than the one due to the change in the bond length.[13] For simplicity, we neglect this effect in the present paper.

The tight-binding Hamiltonian in the presence of the corrugation becomes

$$H=-\sum_{\mathbf{l},\boldsymbol{\delta},\sigma} t[z_{Bl+\boldsymbol{\delta}}-z_{Al}](c^{\dagger}_{lA,\sigma}c_{l+\boldsymbol{\delta}B,\sigma}+\text{H.c.}), \tag{3}$$

where $\boldsymbol{l}=(l_x,l_y)$ denotes the integer coordinates in the hexagonal Bravais lattice and $\boldsymbol{\delta}=\{(0,0),(-1,0),(-1,1)\}$.

B. Dirac equation

A low-energy Hamiltonian can be obtained from Eq. (3) by expanding the Fourier transform of the electron operators around two of the inequivalent points where the dispersion relation vanishes, namely, the Dirac points (DPs). We choose these points as given by $\mathbf{K}=\frac{2\pi}{3a}(1,\frac{1}{\sqrt{3}})$ and $\mathbf{K}'=\frac{2\pi}{3a}(1,-\frac{1}{\sqrt{3}})$. In addition we assume a smooth variation in $z(x)$, i.e., $\tau\gg a$. The low-energy physics is described by the sum of two Dirac Hamiltonians for massless particles in a pseudomagnetic field. It is given by

$$H=v_F\int dr^2\{\boldsymbol{\Psi}_1^{\dagger}(r)\boldsymbol{\sigma}^*\cdot[-i\boldsymbol{\nabla}+\boldsymbol{A}(r)]\boldsymbol{\Psi}_1(r)$$
$$+\boldsymbol{\Psi}_2^{\dagger}(r)\boldsymbol{\sigma}\cdot[-i\boldsymbol{\nabla}-\boldsymbol{A}(r)]\boldsymbol{\Psi}_2(r)\}, \tag{4}$$

where $v_F=\frac{3t_0a}{2}$ is the Fermi velocity, $\boldsymbol{\sigma}=(\sigma_x,\sigma_y)$ is the vector of the Pauli matrices, and $\boldsymbol{\sigma}^*$ its complex conjugate. The two-component field is $\boldsymbol{\Psi}_i=(c_{iA},c_{iB})$ with $c_{i,A(B)}$ creation field operators over the A(B) sublattices. The index $i=1,2$ refers to states with momentum near $\mathbf{K}$ and $\mathbf{K}'$. The gauge vector $\boldsymbol{A}(r)=(A_x,A_y)$ is induced by the rippling and is given by

$$A_x = 0,$$

$$A_y = -\frac{\alpha}{4}(\partial_x h)^2 = -\frac{\alpha}{4}(h_0 q)^2\left[\cos\left(\frac{4\pi}{\tau}x\right)+\frac{1}{2}\right] \equiv \hat{A}_y + k_0, \tag{5}$$

where $k_0 = -\frac{\alpha}{8}(h_0 q)^2$ is the $k=0$ Fourier component of A_y and $q=\frac{2\pi}{\tau}$ the wave vector of the rippling. Note that as the time-reversal symmetry is not broken by the rippling, this implies that the coupling of $\boldsymbol{\Psi}_1$ with $\boldsymbol{A}(r)$ has a different sign than the one of $\boldsymbol{\Psi}_2$. This fact will be important in the study of the nanoribbons undertaken in the next section.

The Dirac equation in a magnetic field corresponding to the one-particle problem generated by Eq. (4) at $i=1$ can be exactly solved for the zero-energy eigenstate. By following similar steps as in Ref. 15 we find the following two degenerate eigenfunctions:

$$\Psi_{+0}(x,y) = \frac{N}{\sqrt{L_y L_x}} e^{-ik_0 y}\begin{pmatrix} e^{F(x)} \\ 0 \end{pmatrix},$$

$$\Psi_{-0}(x,y) = \frac{N}{\sqrt{L_y L_x}} e^{-ik_0 y}\begin{pmatrix} 0 \\ e^{-F(x)} \end{pmatrix} \tag{6}$$

with $F(x)=\frac{\alpha}{8}h_0^2 q \sin(2qx)$ and $L_x(L_y)$ the system length in $x(y)$ direction. N is a normalization constant given by $N=[I_0(\frac{\alpha h_0^2 q}{4})]^{-1/2}$ and I_0 is the modified Bessel function of zero order.

The low-energy eigenstates of Eq. (4) can be studied by degenerate perturbation theory over the zero-energy states $\Psi_{+0}(x,y)$ and $\Psi_{-0}(x,y)$. The potential A_y is periodic with period $\frac{\tau}{2}$. Therefore the solutions of Eq. (4) fulfill the Bloch theorem. They will have the form

$$\Psi_{n,\boldsymbol{k}}(x,y) = e^{i\boldsymbol{k}\cdot\boldsymbol{r}}\psi_{n,k_x}(x), \tag{7}$$

where n is a band index and k_x belong to the Brillouin zone of the imposed periodic lattice, i.e., $-\frac{2\pi}{\tau} \le k_x < \frac{2\pi}{\tau}$. Besides there is no restriction on the values of k_y. Note that Eq. (6) is of the form of Eq. (7) with a quasimomentum of the zero-energy eigenstates given by $\boldsymbol{k_0}=(0,-k_0)$, and a function $\psi_{0,k_x}(x)$ given by

$$\psi_{0,k}(x) = \frac{N}{\sqrt{L_y L_x}}\begin{pmatrix} a_0 e^{F(x)} \\ b_0 e^{-F(x)} \end{pmatrix}, \tag{8}$$

a_0 and b_0 satisfying $\sqrt{a_0^2+b_0^2}=1$. In Eq. (7) the Bloch function fulfills $\psi_{n,k_x}(x+\frac{\tau}{2})=\psi_{n,k_x}(x)$ and satisfies $H(\boldsymbol{k})\psi_{n,\boldsymbol{k}}=E_{n,\boldsymbol{k}}\psi_{n,\boldsymbol{k}}$ with $H(\boldsymbol{k})$ given by

$$H(\boldsymbol{k}) = H_0(\boldsymbol{k}) + H_{int}(\boldsymbol{k}),$$

$$H_0(\boldsymbol{k}) = v_F \boldsymbol{\sigma}^* \cdot [-i\boldsymbol{\nabla} + \hat{\boldsymbol{A}}(\boldsymbol{r})],$$

$$H_{int}(\boldsymbol{k}) = v_F \boldsymbol{\sigma}^* \cdot (\boldsymbol{k} + \boldsymbol{k_0}). \tag{9}$$

As $H_0(\boldsymbol{k})\psi_{0,\boldsymbol{k}}(x)=0$ we identify $H_0(\boldsymbol{k})$ as the unperturbed Hamiltonian. The approximate near-zero-energy eigenstates are obtained by diagonalizing H_{int} in the subspace of the degenerate zero-energy states. H_{int} projected onto this subspace is a 2×2 matrix called $\boldsymbol{h}$ and given by

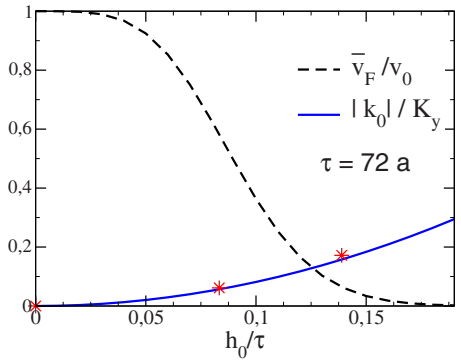

FIG. 2. (Color online) Shifting of the DP $|k_0|$ normalized to the y coordinates of this point (K_y) as a function of h_0/τ (solid line). We also show $\frac{\hat{v}_F}{v_F}$ giving the reduction in the Fermi velocity (dotted line). The results of the numerical calculation on the tight-binding Hamiltonian are shown by stars.

$$\boldsymbol{h} = \hat{v}_F\begin{pmatrix} 0 & k_x + i(k_y + k_0) \\ k_x - i(k_y + k_0) & 0 \end{pmatrix},$$

$$= \hat{v}_F \boldsymbol{\sigma}^* \cdot (\boldsymbol{k} + \boldsymbol{k_0}), \tag{10}$$

$\hat{v}_F = \hat{v}_F(h_0,\tau) = N^2 v_F$ is a renormalized Fermi velocity. The eigenvalues of Eq. (10) are

$$E_1(k_x,k_y) = \pm \hat{v}_F\sqrt{k_x^2 + (k_y + k_0)^2}. \tag{11}$$

We see that the main effects of the corrugation are: (1) DP situated at $\boldsymbol{K}$ has been shifted to $\boldsymbol{K}-\boldsymbol{k_0}$. (2) $\hat{v}_F$ decreases by increasing the rippling.

If we had studied the behavior near $\mathbf{K}'$ by analyzing the second term in Eq. (4) we would have obtained instead of Eq. (11) the result

$$E_2(k_x,k_y) = \pm \hat{v}_F\sqrt{k_x^2 + (k_y - k_0)^2}. \tag{12}$$

Therefore $\boldsymbol{K}'$ moves opposite than $\boldsymbol{K}$. As k_0 is a negative quantity the two DPs move away from each other in presence of the rippling. In Fig. 2 we show the relationships $\frac{|k_0|}{K_y}$ and $\frac{\hat{v}_F}{v_F}$ as a function of $\frac{h_0}{\tau}$.

For completeness, let us provide a comparison of the above findings with the numerically calculated band structure of the corrugated graphene layers within a tight-binding approximation. Since we are trying to detect the displacement of the Dirac points, first we have to compute the band structure for the uncorrugated case. Note here that since the adopted rippling develops in the x direction with a period equal to τ, the unit cell must be extended in order to include the whole period of the rippling. This enlargement of the unit cell produces a reduction in the k_x components of the Dirac points K and K' due to band reflection at the border of the original first Brillouin zone. As can be seen in Fig. 3, where we show the low-energy spectrum obtained for corrugations with period $\tau=72a$, the Dirac point is shifted in the y direction as previously predicted. A quantitative comparison of the shifting obtained numerically and analytically is shown

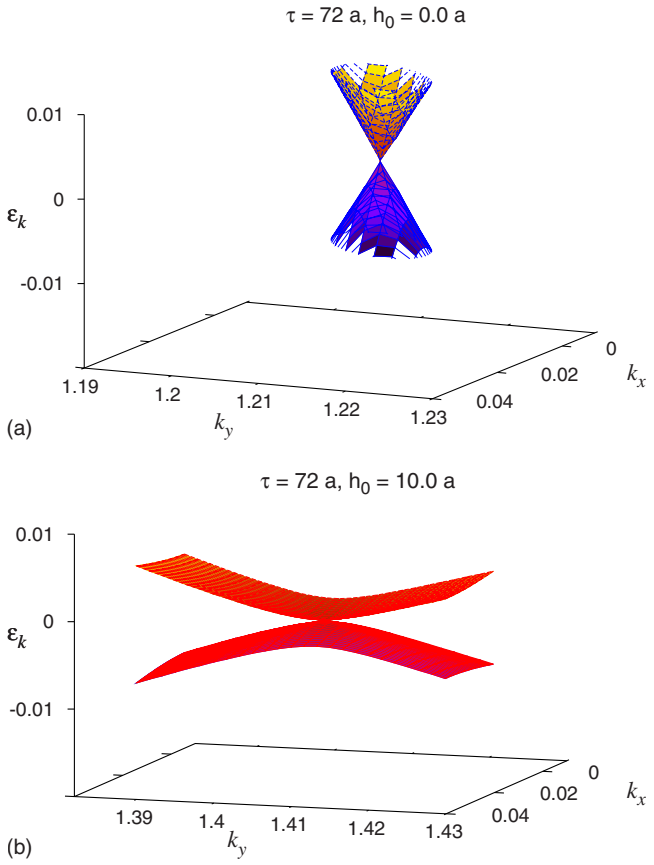

FIG. 3. (Color online) Low-energy band structure of: (a) uncorrugated and (b) corrugated graphene layers. The rippling parameters are displayed in each figure. Note the shift of the DP in (b) with respect to its position in (a). Note also the flattening of the band. Both effects are predicted by the analytic calculation based on the Dirac equation in the presence of a pseudomagnetic field induced by the rippling.

in the Fig. 2. Also, in addition to this shift and in agreement with the previous prediction, the slopes of the dispersion bands decrease for the corrugated graphene implying a reduction in the Fermi velocity for the electrons near the Fermi level. It should be mentioned here that this result is related with the appearance of Landau-type levels (LL) induced by rippling and studied in related works.[11] Note that from Fig. 2 we see that large values of $\frac{h_0}{\tau}$ are required to obtain a total flattening of the band. This could be interpreted as that the predicted zero LL appears only when the rippling is strong enough. This conclusion is consistent with the results of Ref. 12 where it was shown that, as a result of the relaxation of the structure, the corrugation decreases and the flat band disappears from the spectrum.

III. EFFECT OF THE RIPPLING: ARMCHAIR GRAPHENE NANORIBBONS

Let us now turn to the main subject of this work which is the study of the effects of corrugations on the spectra of graphene nanoribbons. As we have mentioned in the introduction, a tight-binding-based description of the electronic properties of the ribbons predicts that, depending on their width and border edge type, they can be metallic, with a zero band gap, or insulators.[8] For example, for the armchair edge (Fig. 1) there are specific values of the width for which metallic behavior is expected. Otherwise they should be insulators. In spite of that, the experiments show that graphene nanoribbons are insulators independently of their width.[9] Though device-fabrication processes do not give atomically precise control on the type of edge, this seems to show that a pure tight-binding model is not enough to describe the GNR as it does for the sheets. Both electronic correlations[16] and edge disorder[17,18] have been proposed as possible mechanisms that give rise to this behavior. In this section we show that the rippling can give an additional source for the electronic gap, at least for the armchair-edge type.

A. Dirac equation with boundary conditions

As for the infinite graphene sheet, it is possible to study the low-energy electronic structure of graphene nanoribbons by a Dirac-type equation, but in this case adequate boundary conditions must be imposed.[8] For the uncorrugated armchair edges, the valley states near the DPs, **K** and **K′**, get mixed and metallic behaviors are obtained for certain widths.

The exact solutions of the Dirac equations in a confined geometry and in presence of the rippling is, in general, not possible. Instead, we assume that the approximations used in the previous section for the low-energy states are also valid when the adequate boundary conditions for an AGNR are taken into account. Specifically, we take Hamiltonian (10) with the replacement $\boldsymbol{k} \rightarrow -i\boldsymbol{\nabla}$ as the approximated one for the low-energy states near $\boldsymbol{K}$ of a ribbon. For the states near $\boldsymbol{K}'$ we replace $\boldsymbol{\sigma} \rightarrow \boldsymbol{\sigma}^*$ and $-\boldsymbol{k}_0 \rightarrow \boldsymbol{k}_0$. We solve these equations by following similar steps as the ones used for the flat nanoribbons in Ref. 8. This approximation is enough to obtain a quantitative agreement with the results of numerical solution for the tight-binding model (see below).

The wave functions for sublattices A(B) are given by

$$\Phi_{A(B)}(\boldsymbol{r}) = e^{i(\boldsymbol{K}-\boldsymbol{k_0})\cdot\boldsymbol{r}}\Psi_{1,A(B)}(\boldsymbol{r}) + e^{i(\boldsymbol{K}'+\boldsymbol{k_0})\cdot\boldsymbol{r}}\Psi_{2,A(B)}(\boldsymbol{r}), \tag{13}$$

where $\Psi_{1,A(B)}$ are the components of the spinor wave functions for states near $\boldsymbol{K}$ and $\Psi_{2,A(B)}$ the ones near $\boldsymbol{K}'$. For the AGNR the wave function should vanish at $y=0$ and L_y. Translational invariance in the x direction is preserved for the low-energy state accounted by our approximate treatment. Therefore $\Psi_{1(2),A(B)}(\boldsymbol{r})$ can be written as

$$\Psi_{1(2),A(B)}(\boldsymbol{r}) = e^{ik_x x}\phi_{1(2),A(B)}(y). \tag{14}$$

The solutions of the Dirac equation with the previous stated boundary conditions have now the form

$$\phi_{1,B} = e^{ik_n y},$$

$$\phi_{2,B} = -e^{-ik_n y} \tag{15}$$

with the energies given by

$$\epsilon = \pm \hat{v}_F\sqrt{k_x^2 + k_n^2}. \tag{16}$$

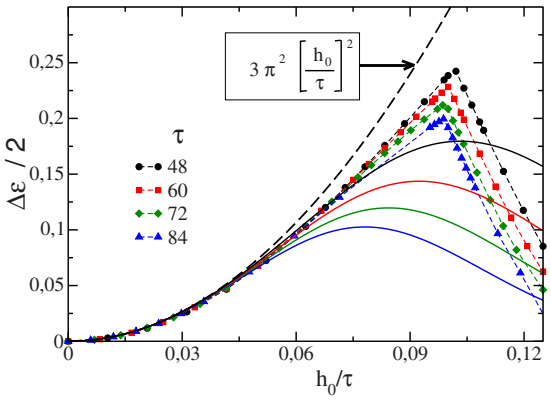

FIG. 4. (Color online) Behavior of the zero-energy gap as a function of h_0/τ in corrugated armchair graphene nanoribbons. Solid lines are analytic results from a Dirac equation. The values obtained from band-structure calculations are showed by weak dotted lines and the points. The strong dotted line is the quadratic behavior predicted for small corrugation (see text for details).

The values of k_n fulfill $\sin[(k_n+K_y-k_0)L_y]=0$ and are given by

$$k_n = \frac{n\pi}{L_y} - K_y + k_0. \tag{17}$$

In absence of k_0, k_n could vanish giving rise to a gapless spectrum as seen from Eq. (16). This is the case when the width of the ribbons is $L_y=3(n_y-1)\sqrt{3}a$ with n_y integer. However, when k_0 is present the condition for a gapless spectrum cannot be fulfilled in general. Even more, for the L_y which gives a gapless spectrum in absence of the rippling, we now have a dispersion of the form $\epsilon=\pm\hat{v}_F\sqrt{k_x^2+k_0^2}$ and therefore a gap given by

$$\frac{\Delta\epsilon}{2} = 2\hat{v}_F k_0. \tag{18}$$

As discussed in the previous section, for $\frac{h_0}{\tau}\ll 1$ the Fermi velocity does not renormalize. Thus, we expect that the gap will behave as

$$\frac{\Delta\epsilon}{2} = 3\pi^2\left(\frac{h_0}{\tau}\right)^2. \tag{19}$$

A universal quadratic dependence of the gap with $\frac{h_0}{\tau}$ is predicted. For greater values of $\frac{h_0}{\tau}$, v_F acquires an extra dependency on h_0 separating from a simple quadratic law. All these results are shown in Fig. 4 together with numerical results to be discussed in the following. Note that for stronger corrugation $\hat{v}_F$ goes to zero, which has been associated with the appearance of a pseudo-LL. Thus, for such value the gap should vanish.

To confirm the previous predictions we have calculated numerically the eigenstates of corrugated armchair graphene nanoribbons. This was performed following the steps described at the end of Sec. II taking into account here the armchair ribbon geometry displayed in Fig. 1. As we were interested in the detection of the gap and in analyzing its dependency with the corrugation, we have explored a wide set of rippling parameters keeping fixed the width of the ribbons at the values in which they possess metallic behavior in absence of corrugation.

Figure 4 shows the zero-energy gap as a function of h_0/τ for the various sets of parameters displayed on the plot, for a width given by $n_y=8$. Note that for the small values of h_0/τ included in this figure, the gap does not depend on h_0 and τ independently but on the ratio of these quantities. In this figure we have also included the law defined by Eq. (18). Note that the analytic approach predicts very well the values of the gap when the corrugation is small. When the corrugation increases our low-energy approximation is less precise. Note, however, that the overall behavior is well reproduced. In particular the closing of the gap is accounted for stronger corrugations.

B. Quantum conductance

Finally, we analyze how all the above findings affect the electronic transport properties of the armchair graphene nanoribbons. For this purpose, we have employed the nonequilibrium Green's function formalism[14,16] which provides a useful method to study the quantum conductance in nanoscopic systems.

Before we give a discussion of the results, let us present a brief description of the method and the implementation adopted. We considered one corrugated unit cell, as central region H_C, connected to two semi-infinite graphene nanoribbon flat leads. The three parts of the system have a width of $n_y=8$ which corresponds to a zero band-gap structure in the uncorrugated case. The hopping parameter in the Hamiltonians of both leads, H_L and H_R, is t_0. Hence, the whole system is then described by

$$H = H_C + H_R + H_L + h_{LC} + h_{LR}, \tag{20}$$

where h_{LC} and h_{LR} are the hopping terms from both leads to the central corrugated portion of the nanoribbon, which we set equal to t_0 [see Fig. 1(a)]. Within this formalism, the Landauer conductance $G(E)$ of the system, in a zero-bias approximation, is expressed as

$$G(E) = \frac{2e^2}{h}T(E), \tag{21}$$

where $T(E)$ is the transmission function given by $T(E)=\mathrm{Tr}[\Gamma_L(E)\mathcal{G}_C(E)\Gamma_R(E)\mathcal{G}_C^\dagger(E)]$, with $\Gamma_\ell=-2\mathcal{I}m[\Sigma_\ell(E)]$ $(\ell=L,R)$ being the couplings of the corrugated graphene nanoribbon to the leads, and $\mathcal{G}_C(E)=(E-H_C-\Sigma_L-\Sigma_R)^{-1}$ the total Green's function including the leads self-energies, Σ_L and Σ_R. These self-energies must be calculated through the leads surfaces Green's functions (SGF). Although it was reported a very time-efficient way to compute the SGF of graphene nanoribbons leads (see Fig. 2 of Ref. 19) for the sake of simplicity we implemented the recursive iteration procedure, given by $g_\ell=(E-H_\ell-T_\ell^\dagger g_\ell T_\ell)^{-1}$, where H_ℓ is the unit-cell lead Hamiltonian and T_ℓ is the interlayer coupling in the semi-infinite lead. For the small width nanoribbons studied here we have checked that a fast convergence is obtained. In the iterative procedure, we have set the tolerance as 10^{-6}.

Figures 5(a)–5(c) show the transmission coefficients obtained for armchair-border-type nanoribbons whose period τ

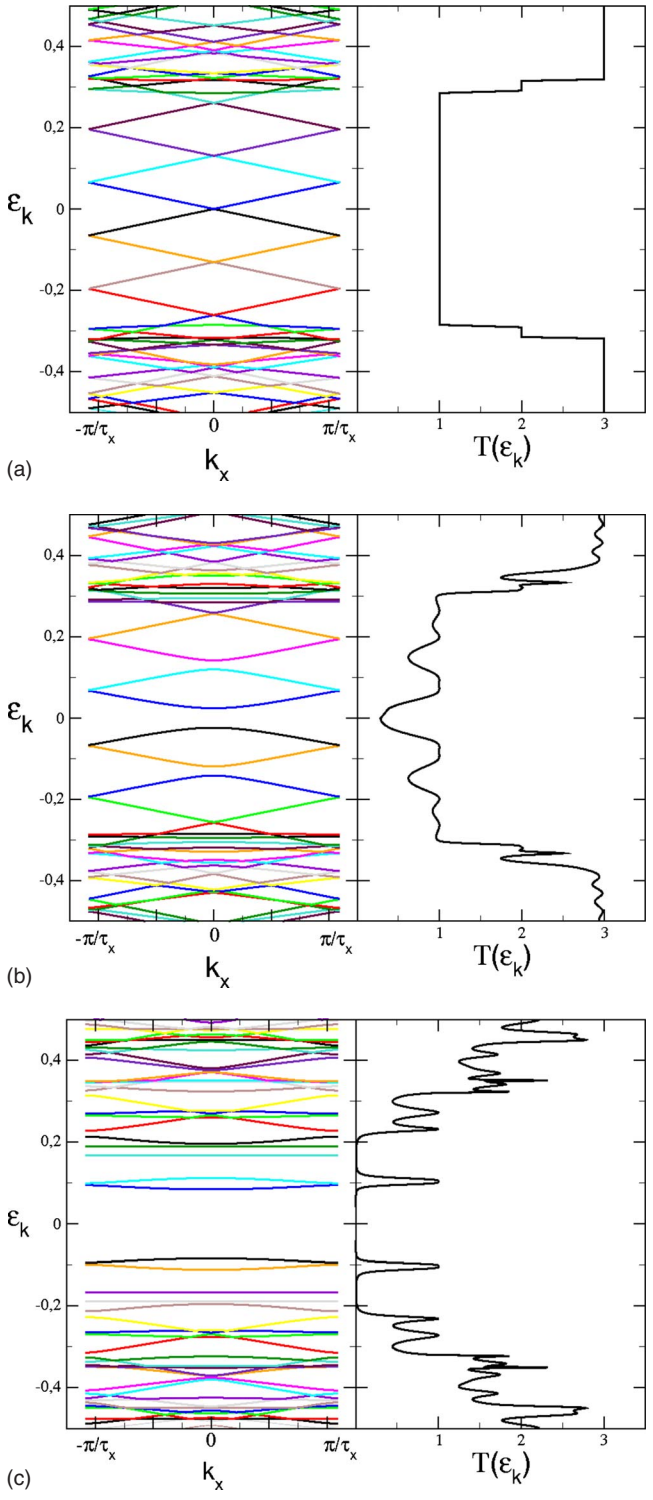

FIG. 5. (Color online) Transmission coefficient of corrugated armchair graphene nanoribbons. n_x=24, n_y=8 and (a) h_0=0, (b) h_0=3, and (c) h_0=6 in units of a. In each left panel we included the corresponding low-energy band structure, which serve to a better analysis of the behavior of $T(E)$.

is 72a and with amplitudes h_0=0.0, 3.0, and 6.0 in units of a, respectively. In the left panels of the plots we included the corresponding low-energy band structures computed numerically following the description given at the end of Sec. II suited for the nanoribbon case. The band reflection at the first Brillouin zone can be clearly seen in Fig. 5(a), which corresponds to the uncorrugated case. Here, and such as is expectable, the transmission coefficient is equal to one at the Fermi energy. In Fig. 5(b) the band gap at the Fermi energy appears and according to this the transmission is reduced. The fact that it does not reach zero is produced because the central region possesses only one corrugated unit cell. Increasing the amplitude of the rippling the gap becomes broader as observed in Fig. 5(c) and the transmission goes to zero around the Fermi energy. These results are consistent with the ones obtained above by solving the Dirac equation. Here, also a second null conductance region appears above a thin perfect conductance interval at higher energies. In addition to these results, obtained by keeping τ_x fixed and varying h_0, we calculated $T(E)$ for a wide range of corrugation periods and amplitudes, finding in all cases the appearance of a gap at low energies around E_F.

IV. CONCLUSIONS

After having analyzed the Dirac equation including the pseudomagnetic field induced by the corrugation and having explored numerically a wide realistic range of corrugations, we have found that the corrugation produces a gap in the low-energy electronic spectrum of otherwise conducting armchair graphene nanoribbons. We have found that this gap scales quadratically with the rate between the height and the wavelength of the deformation. According to this, the quantum conductance $G(E)$ of the ribbons, calculated by the NEGF formalism, vanishes around the Fermi energy of undoped corrugated samples.

These results were preceded by an analysis of the corrugation effects over the electronic spectra of graphene layers. There, we have found that the corrugation just shifts the Dirac points and renormalizes the Fermi velocity. These findings are in agreement with the results of numerical calculations.

In view of this, we conclude that the corrugation is an important source of gap in the spectra in addition to the electronic correlations to which this effect is typically assigned.[16] Although our study was performed modeling the corrugations by single sinusoidal functions, since any lattice deformation could be approximated quite well by an adequate sum of sines, we strongly believe that the results obtained here are extensible to general corrugations. Moreover, our findings could be revealed in future experiments undertaken on suspended clean samples[20] in which extrinsic effects would be minimized. For these reasons we expect that our paper motivates experimental works to determine the dependency of the gap with the corrugation parameters that can be varied by changing the applied stress[21,22] or the temperature.

ACKNOWLEDGMENTS

We thank D. Mastrogiussepe for a carefull reading of the manuscript. This work was supported in part by Grant No. PICT 1647 (ANPCYT).

[1] K. S. Novoselov, A. K. Geim, S. V. Morozov, D. Jiang, Y. Zhang, S. V. Dubonos, I. V. Grigorieva, and A. A. Firsov, Science **306**, 666 (2004).
[2] A. H. Castro Neto, F. Guinea, N. M. R. Peres, K. S. Novoselov, and A. K. Geim, Rev. Mod. Phys. **81**, 109 (2009).
[3] M. J. Bowick and A. Travesset, Phys. Rep. **344**, 255 (2001).
[4] J. C. Meyer, A. K. Geim, M. I. Katsnelson, K. S. Novoselov, T. J. Booth, and S. Roth, Nature (London) **446**, 60 (2007).
[5] S. V. Morozov, K. S. Novoselov, M. I. Katsnelson, F. Schedin, L. A. Ponomarenko, D. Jiang, and A. K. Geim, Phys. Rev. Lett. **97**, 016801 (2006).
[6] E. Kim and A. H. Castro Neto, EPL **84**, 57007 (2008).
[7] M. I. Katsnelson and A. K. Geim, Philos. Trans. R. Soc. London, Ser. A **366**, 195 (2008).
[8] L. Brey and H. A. Fertig, Phys. Rev. B **73**, 235411 (2006).
[9] M. Y. Han, B. Ozyilmaz, Y. Zhang, and P. Kim, Phys. Rev. Lett. **98**, 206805 (2007).
[10] A. Cresti, N. Nemac, B. Biel, G. Niebler, F. Triozon, G. Cuniberti, and S. Roche, Nano Res. **1**, 361 (2008).
[11] F. Guinea, M. I. Katsnelson, and M. A. H. Vozmediano, Phys. Rev. B **77**, 075422 (2008).
[12] T. O. Wehling, A. V. Balatsky, A. M. Tsvelik, M. I. Katnelson, and A. I. Lichtenstein, EPL **84**, 17003 (2008).
[13] J. W. Klos, A. A. Shylau, I. V. Zozoulenko, H. Xu, and T. Heinzel, Phys. Rev. B **80**, 245432 (2009).
[14] S. Datta, *Electronic Transport in Mesoscopic Systems* (Cambridge University Press, Cambridge, 1995) (paperback edition, 1997).
[15] I. Snyman, Phys. Rev. B **80**, 054303 (2009).
[16] H. Santos, L. Chico, and L. Brey, Phys. Rev. Lett. **103**, 086801 (2009).
[17] T. C. Li and S.-P. Lu, Phys. Rev. B **77**, 085408 (2008).
[18] E. R. Mucciolo, A. H. Castro Neto, and C. H. Lewenkopf, Phys. Rev. B **79**, 075407 (2009).
[19] R. Golizadeh-Mojarad, A. N. M. Zainuddin, G. Klimeck, and S. Datta, J. Comput. Electron. **7**, 407 (2008).
[20] K. I. Bolotin, K. J. Sikes, J. Hone, H. L. Stormer, and P. Kim, Phys. Rev. Lett. **101**, 096802 (2008).
[21] E. Prada, P. San-Jose, G. Leon, M. Fogler, and F. Guinea, arXiv:0906.5267 (unpublished).
[22] V. M. Pereira, A. H. Castro Neto, and N. M. R. Peres, Phys. Rev. B **80**, 045401 (2009).